Proceedings World Geothermal Congress 2020+1
Reykjavik, Iceland, April - October 2021

Reservoir Seismic Imaging Using an Elastic Full-wave Inversion Approach Applied to Multi-OVSP Data in the Context of Soultz-sous-Forêts

Christophe Barnes[1,2], Yassine Abdelfettah[1], Nicolas Cuenot[3], Eléonore Dalmais[3] and Albert Genter[3]

[1] Geophysical Inversion & Modeling labs, 57 allée de l'Albatros 95800 Courdimanche – France. [2] University of Cergy-Pontoise, Neuville/Oise – France. [3] ES-Géothermie, 5 Rue de Lisbonne 67300 Schiltigheim – France.

christophe.barnes@gim-labs.com

Keywords: Full wave inversion, OVSP, Fault imaging, EGS, Soultz-sous-Forêts

ABSTRACT

In the present paper, we consider the context of Soultz-sous-Forêts geothermal site (France), revisiting well seismic data acquired in 2007. We will apply a full-wave inversion method on the offset vertical seismic profiles in order to detect or image the heterogeneities and the faults in the granite geothermal reservoir. The main goal of this study is both to evaluate the application of a method already used in the oil&gas industry to geothermal purpose and if successful, to improve the knowledge of the fault network at the reservoir level.

We recall that, in a crystalline context, the 3D geometry of the fracture/fault network in the granite around and between the wells is a critical issue in order to well constrain the fluid flow modeling in the reservoir and thus to help optimizing the geothermal production.

The proposed full-wave inversion method (FWI) has already been conducted with success on offset VSP data (North Sea gas reservoir). However, such seismic imaging and characterization have been performed essentially in sedimentary contexts. Applying the FWI method to structures like faults in a crystalline environment is a real challenge. A previous study on these OVSP data has shown that waves scattered from the interaction of the incident seismic wave with the main faults is actually recorded at the receivers (3C geophones, P-to-S conversion for instance). Information is then present in the seismic data. The full-wave approach being more accurate than standard seismic processing methods, we expect an improvement of the knowledge of the reservoir structure, and particularly, of the main faults network.

In this paper, we develop first the methodology of the FWI. The main features are the multiscale approach using increasing frequency bands and spatial correlations, and that the rheology used to model the seismic wave propagation is realistic and accurate. The physics of seismic wave propagation is then correctly reproduced, allowing to extract more information from the seismic data. In addition, it allows to obtain several field parameters as the P-wave and S-wave velocities and others, depending on the case. As the computation costs are very high due to the accurate seismic fullwave modeling, we could consider a 2.5D seismic wave propagation in the upper part of the model, while in the granite reservoir both field parameters and the propagation are fully 3D.

1. INTRODUCTION

In exploration of a deep geothermal resource, the location of a heat anomaly can be a first key for a success of a deep geothermal project. In addition, several other parameters could play a major role in project success or failure. Porosity, permeability, geomechanical stress and heat flow could undoubtedly play an important role as well. Among these parameters, fracturation and faulting, inducing the secondary permeability is a critical parameter particularly in enhanced geothermal systems (EGS). It plays a main role to increase the rock/fluid surface establishing a natural heat exchanger, and thus to drive a deep hot water to reachable and exploitable depth.

Fracturation and fault characterization for deep geothermal reservoir remain a very difficult task. From the surface, we can mainly identify major and important faults related to the reservoir. From the well, once drilled, the fault network which could cross our geothermal reservoir can be investigated by deriving structural information about nearby faults from induced microseismic studies (Dorbath et al., 2009). These regional faults could have an important positive and or negative effect on geothermal reservoir and then on the feasibility of a geothermal project. These faults could be well delineated by classical geophysical techniques for instance seismic reflection (Richard et al., 2019), gravity and magnetotelluric (Abdelfettah et al., 2019a, 2019b), and then their contribution on the geothermal reservoir could be assessed. However, intermediate and local faults belonging to the same fracture network show more characterization challenges. For the case of a deep reservoir, as these faults are generally located in the deeper part, their identification and vertical extension from surface remain difficult and, in some cases, impossible.

A complementary solution is to use seismic borehole data once a first well has been drilled. The Multi-Offset Vertical Seismic Profiling (OVSP) is appropriate as walkaway or 3D-VSP because multi-offset seismic data allows to extend the reservoir imaging and characterization a few hundred meters around the well. The key idea is to acquire several VSP with different azimuth and offset according to the target. The combination of these OVSPs could provide a better image and enhance borehole seismic imaging. As seismic waves cross the weather zone (WZ) only one times, the VSP (and OVSP) technique show generally a higher frequency content and a better signal amplitude and a high S/N ratio compared to standard surface seismic. Moreover, the illumination is good in the well vicinity and the heterogeneities in the reservoir located near the well will scattered P- and S-wave near receivers allowing a better resolution in the well vicinity. The challenges in fracture identification decrease when using this high-resolution technique. However, the wave-field is more complex than for surface seismic data as receivers record up- and down-going wave, P-

and S- reflected waves, P-to-S and S-to-P conversion, i.e. much more than primary reflections. The drawback is that conventional processing often fails to extract all the information present in the recorded wavefield.

Promising trials of applying FWI methods to offset well seismic data have been carried out (e.g. Charara et al., 1996; Hirabayashi and Leaney, 2006; Roberts and Hornby, 2007; Barnes et al., 2009 and 2010; Podgornova and Charara, 2011; Owusu et al., 2016). These OVSP studies applied to oil and gas challenges like subsalt imaging, imaging below screen, velocity estimation for pore pressure detection or CO_2 sequestration shown the added value of using this high-resolution exploration technique. In deep geothermal, VSP has been successfully applied to characterize fractures in and neighbouring granitic reservoir in Soultz-sous-Forêts (e.g. Place et al., 2010; Sausse et al., 2010). A synthetic study done in the granite geological context showed a high potential of the OVSP for fractures characterization (e.g. Reiser et al., 2017). The VSP data analysis was always done by a classical approach using mainly wave field separation to up- and down- fields. This approach gives good results in sedimentary context, but much less in a granite context hidden by a thick sedimentary cover as in Soultz.

In this paper, we showed that the Full Wave Inversion (FWI) approach could improve fractures identification and analysis in granite context.

2. GEOLOGICAL SETTING

Soultz-sous-Forêts which belongs to the Upper Rhine Graben (URG), is characterized by a thermal anomaly (Pribnow and Schellschmidt, 2000). It is very well documented by several previous geological and geophysical studies. These studies concern in the beginning the oil exploration and production (e.g. Sittler, 1972) and more recently geothermal exploration and production for heat and electricity generation (e.g. Genter et al., 2010; Baujard et al., 2018). The northern part of the URG shown a global E-W extension started from the Eocene (e.g. Edel et al., 2006). The today stress regime is NW-SE compression yield to strike slip mechanisms for the existing faults and fractures (e.g. Valley and Evans, 2007).

The geological structures are nearly vertical and comprise sediments and basement. The sediments include Quaternary, Pliocene, Oligocene, Eocene and Paleocene from Cenozoic, and Lias and Dogger for Jurassic, Keuper, Muschelkalk and Buntsandstein for Triassic (e.g. Aichholzer et al., 2016). The structures show a main N-S strike according to the graben extension, and NNE-SSW strike in the northern part close to German-France border. The top of the granitic basement could be reached only at around 1400 m (MSL) under GPK1 well-head. Detailed fracture studies done on continuous core samples or from borehole image logs acquired in the Soultz wells show a NNW-SSE dominating strike orientation (Dezayes et al., 2010).

Several major faults with N-S global extension cross our studied area (e.g. Soultz-sous-Forêt, Rittershoffen and Kutzenhausen faults and other faults). Several many other secondary faults and fractures with different orientation could be found making a connection with the main faults. The granite in Soultz-sous-Forêts is relatively fractured to highly fractured in specific depth, for instance at 1810 m, at 2840 m and 3500 m in the GPK1 well (Dezayes et al., 2010). In Soultz-sous-Forêts, a granite matrix porosity below 1%, whereas it reaches 20% for a fractured and altered granite (Genter et al, 2000). This secondary porosity increases shown that the granite could be highly fractured. A detailed fractures and fault analysis in the Soultz boreholes of Soultz namely GPK1, GPK2, GPK3, GPK4 and EPS1 using borehole imaging techniques as well as data logging could be found in Genter et al. (1997) and Dezayes et al. (2010). Natural fractures which are generally clustered, define hydrothermally altered and fractured zones made of a core part surrounded by a clay-rich damaged zone (Genter et al., 2000). Such fractured zones could be permeable (or not) and are locally bearing natural geothermal fluids very salty (Sanjuan et al., 2016). However, it is very difficult to extrapolate fracture/fault extension by using borehole data only (Genter et al., 1997; Sausse et al., 2010). It is the reason why the reprocessing of VSP data collected at Soultz using an elastic full-wave inversion approach could significantly contribute to improve our structural knowledge of the fault system close to the Soultz geothermal wells.

3. METHODOLOGY

When applied to borehole seismic, the conventional imaging tool, the migration, has to overcome the problem of lack of redundancy compared to surface seismic. This is a common problem for any context. Moreover, for the fault imaging goal, the conventional technique of downgoing and upgoing waves separation is no longer usable as the medium is not layered and the object geometry is far from sub-horizontal structures. In addition, the deconvolution of upgoing waves by downgoing wavefield is approximative when using offset borehole seismic data. The FWI method does not suffer from the above limitation except the weak redundancy which can be overcome by using additional constraints in the inversion process.3.1 The inverse problem applied to seismic data

The inverse problem can be expressed as the minimization of a misfit function (Tarantola, 1987). For least squares, this function is a scalar function defined over the model space as:

$$S(\mathbf{m}) = \Delta\mathbf{d}^{\mathbf{T}}\mathbf{C}_{\mathbf{D}}^{-1}\Delta\mathbf{d} \qquad (1)$$

where $\mathbf{m}$ is a model, $\Delta\mathbf{d} = \mathbf{g}(\mathbf{m}) - \mathbf{d}_{obs}$ are the residuals with $\mathbf{d}_{obs}$ the observed data, and $\mathbf{g}(\mathbf{m})$ the synthetic data obtained by simulation of the wave equation, and where $\mathbf{C_D}$ denotes the covariance matrix over the data space. This matrix can be not diagonal as when using the polarization constraint (Charara and Barnes, 2019). The misfit function measures the discrepancy between observed and calculated seismic data, i.e. between amplitude of the signal for each trace. Because of the non-linearity and the complexity of the forward modeling, the misfit is reduced iteratively using a local method based on derivative (Tarantola, 1987). Here, the descent algorithm is based on the conjugate gradient method proposed by Polack and Ribière (1969).

3.2 Modeling the seismic wave propagation

The direct problem associated to the present fullwave inverse problem is the propagation of (visco)elastic waves in an (an)isotrope medium. As the imaging target, i.e. the fault network, is one or several 3D objects in a 3D nearly homogeneous medium, we aim at achieving a 3D inversion. However, as a first step, we will consider a 2D wave propagation for the synthetic experiments used in

the sensitivity analysis (see section 5) and a 2.5D wave propagation for the real data inversion. The 2.5D can be achieved by lateral invariance or as here by symmetry of revolution. These techniques allow us to approximate the 3D green function when the 2D propagation cannot.

3.3 The rheology issue

The actual rheology is elastic for the synthetic FWI experiments in section 5.1 and viscoelastic for the case of real seismic data FWI. When the data redundancy is weak as for borehole seismic, we need to extract the most information from the data. In order to achieve this goal, we must reduce all the additional noises: numeric, experimental, physical, Barnes and Charara (2015). As a rule of thumbs, all these noises should be lesser than the data noise in order to extract information and reduce artefacts. Non additive structures noises have the largest impact on the results (Barnes and Charara, 2015) and reducing the noise due to an inadequate physical law is the main issue. E.g. using a simplified rheology as acoustic, even for marine data, imply large artefact in the solution due to the wrong modeled AVO as shown by Barnes and Charara (2009).

As borehole seismic data generally exhibit a very informative wavefield containing energetic 2nd or even 3rd order scattered waves (Barnes and Charara, 2010). For example, downgoing P-to-S converted waves can convert back to P-wave after reflexion on an interface. P-to-S conversions increase in amplitude according to the offset. As a consequence, in most cases for borehole seismic with offset (OVSP, walkaway, 3D-VSP) and in sedimentary context, once removing the downgoing direct P-wave 80% of the energy is provided by the S-waves (Barnes and Charara, 2010). The elastic rheology is then required.

Moreover, equation (1) is based on amplitude, thus seismic attenuation, often present in the data, should be taken into account as well, at least in the FW modeling (without inverting for attenuation parameters). Anelastic phenomena can be modeled by viscoelasticity at the scale of the seismic wavelength. One often defines a global Q-factor using a constant Q or a nearly constant Q (NCQ) model (Blanch et al. 1995, Christensen, 1982) or even a more general standard linear solid model (SLS). Charara and Barnes (2000, 2004) have proposed to model the attenuation by using two Q-factors, the Q_κ factor related to the bulk incompressibility modulus κ and the Q_μ factor related to the shear modulus μ. The first one is affected by fluids, in particular, liquid-gas mixing while the latter one is related to microstructures of the solid. In FWI, the viscoelastic parameter fields provided poor spatial resolution information as the seismic attenuation is an integrative phenomenon but, when taking into account the seismic attenuation, it allows to obtain a better resolution on other parameters (see for example Barnes et al, 2014 or Charara and Barnes, 2017).

In order to model the wave propagation in the time domain for a viscoelasticity medium, we used the techniques of the strain memory variables (Emmerich and Korn, 1987; Carcione, 1990; Charara et al., 2000).For the viscoelastic inversion, the Fréchet derivatives for the viscoelastic parameters have similar expressions to those for the elastic case (Tarantola, 1988), i.e., a correlation at zero lag between two fields (Charara et al., 2000).

3.4 The discretization of the (visco)elastic wave equation

The finite differences method is based on the displacement form of the wave equation for the viscoelastic rheology. The spatial discretization is using a staggered grid, a 2nd order Taylor expansion explicit scheme in time and 4th order differential operators in space.

3.5 The workflow used for the sensitivity analysis

We consider several cases in order to check the sensitivity and compare the obtained results. The synthetic experiments allow us to check the resolution depending:

- on the fault location: crossing the antenna in the upper part, in the lower part, not crossing the antenna,
- on the fault dip: dip angle and NE/SW directions,
- on the thickness of the fault: 10, 20, 40 m,
- on the physical parameter values drop in the fault zone (20% for velocities, 5% for density),
- on the number of shots,
- on the length of the antenna (and thus the number of receivers),
- on the data frequency range,
- on inversion parameters (spatial correlation, correlation between parameters, polarization).

In this paper, we present only the case crossing the antenna in the lower part with a dip of 70° towards NE, a thickness of 20 m and a decrease of 15% for velocities and 5% for the density in the fault zone.

The synthetic inversion procedure is the following:

1. We consider one of the cases, i.e. a model with a fault and a given acquisition geometry. This model is called the true model, it is used for observed data modeling and it is the model we want to retrieve using the inversion synthetic procedure.
1. We model the “observed” data from the true model. These observed data will be used as data to be inverted in the inversion procedure.
2. We define the same starting model for all cases. This model is used as first model in the iterative non-linear inversion procedure. This starting model is the same model as the true model but without the fault. We consider then the case where all is known perfectly except the fault characteristics (geometry and physical parameters).
3. We run the full-wave inversion from the starting model and the observed data.
4. We obtain the estimated model from the inversion process after some iterations.
5. We compare the estimated model to the true model.

4. GEOPHYSICAL AND GEOLOGICAL DATA

4.1 Offset VSP data

In the purposes, we focus the study on the GPK4 geothermal borehole of Soultz-sous-Forêts. The data were acquired in 2007 by GEIE in the frame of Soultz-sous-Forêts scientific consortium. The data were acquired using four components (4C), following X, Y, Z and hydrophone H. In the total, 26 shots (vibrating point) with offsets varying from a few hundred meters to 5 km with different azimuths have been acquired in GPK3 and GPK4 wells (e.g. Lubrano, 2013).

We consider here only the A0 vibrating point located 180 m NE from the well GPK4 and the antenna located in GPK4 borehole (the data with the best quality). The experiment and corresponding acquired seismograms are named GPK4-A0. The data start from 432 m depth MSL down to 4085 m with an antenna of 187 receivers spaced every 20 m, except for the check-shots (interval is 100 m). The sweep covered a frequency range of 8-88 Hz. The data presented in Figure 1 showed a good SNR except for the first 40 geophones. The downgoing phase with an apparent velocity higher than the direct P (see Figure 1) is likely a reflection on a fault as it has been qualitatively interpreted by Lubrano (2013). One of the goals of the reprocessing of these data using FWI is to obtain quantitative information about the fault from these data (e.g. delineation, thickness, values of physical parameters).

4.2 Geological and geophysical models

From a previous study, a regional 3D geological model covering the northern Alsace including Soultz-sous-Forêts geothermal zone is available. This model was built from the reprocessing of seismic data acquired in the 80's (Maurer et al., 2016) in the frame of EGS Alsace and ANR Cantare programs. Due to the parameters used at this time, with the target was the tertiary layers potentially bearing oil, and scarce information of seismic velocities, this model has uncertainty at the sediment – basement interface that could reach up to several hundred meters, especially in the deepest part of the graben. The first order faults as well as some major sedimentary geological layers as "schistes à Poissons", Tertiary unconformity, top Trias, top Muschelkalk, and top Buntsandstein have been mapped in 3D.

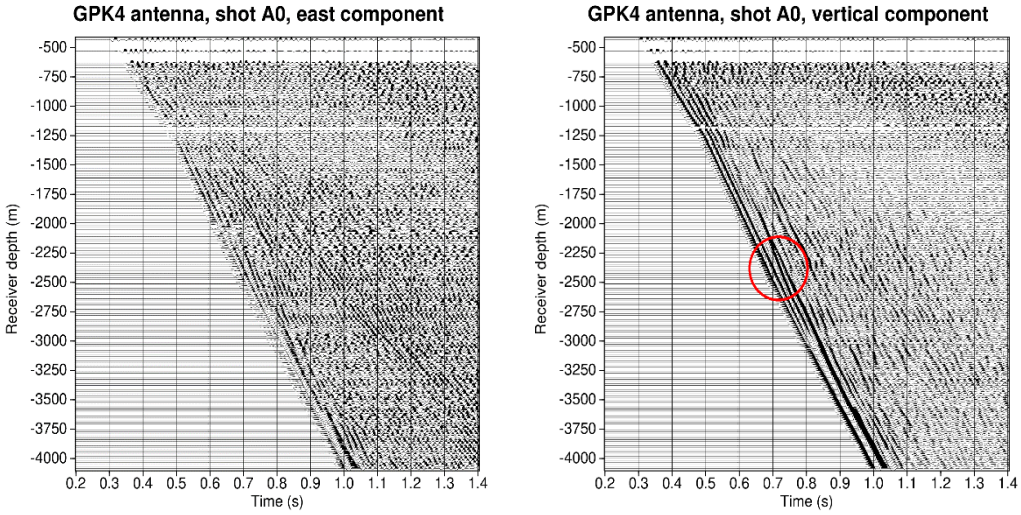

Figure 1: Seismogram of the shot A0 for geophone located in well GPK4. Left: horizontal component (east), P-to-S converted downgoing waves can be noticed. Right: vertical component, in the red circle, the downgoing phase with an apparent velocity more rapid than the direct P has been interpreted as a reflection on a fault crossing the well at 3200 m depth, see for instance Lubrano (2013) and Place et al., (2010).

To build an initial compressional and shear velocity (Vp and Vs) models as well as density model, we performed a review of the existing information. These are mainly derived from borehole data, but also from other models built in previous and different studies. All these models are summarized in Figure 2.

The physical models, i.e. P and S velocities and density fields, are built on the basis of an existing 3D geological model. These physical parameters are defined at the top and the bottom of each geological unit. Following the models showed in Figure 2, these values are interpolated depending if there is a vertical gradient or not.

5. THE SENSITIVITY STUDY

The sensitivity study has been performed using a synthetic data inversion process. We aimed to quantify the ability of the OVSP to identify and characterize fractures in the deep granite.

To perform this sensitivity study, we consider an experiment setup which fit the real OVSP experiment with comparable conditions, for instance we choose the same cross-section orientation, the same source position, and the location of the well-head as well as the wellpath where geophones are located. In addition, we use the seismic velocities and the density models extracted from the 3D models (section 4.2).

5.1 The modeling experiments

The synthetic experiment setup is showed in Figure 3. The idea is to simulate the direct seismic response of a geological model where a fault is present. The orientation and the thickness of this fault are comparable to realistic faults derived from a geological information of Soultz-sous-Forêts. As the major observed faults in GPK4 are subvertical (e.g. Dezayes et al., 2010), we choose a 80° dipping fault zone with a vertical extension, and 20 m for its thickness, which remain a realistic thickness as documented in GPK4 welldata (e.g. Genter et al., 2010). The fault is straight, and the vertical extension of the fault is 1 km. The physical parameter values are smaller in the fault zone. According to the sonic, S-wave and density logs (e.g. Lubrano, 2013), we consider that both velocities can be 25% less and the density 10% less.

To model the VSP data, we consider the 187 receivers of the GPK4-A0 real experiment (section) from -432 m down to -4085 m (MSL) as shown in Figure 3, and a seismic source at 180 m offset. We consider a dominant frequency of 50 Hz, we recorded 2 s using a sampling rate of 1 ms. The results of the fullwave modeling, the synthetic seismograms, are shown in Figure 4. The wavelength of the P wave is about 120 m, however, even if the fault zone thickness is 20 m, the effect on the data are noticeable. Nevertheless, in noisy condition, faults effect on data can be too small for the fullwave inversion technique.

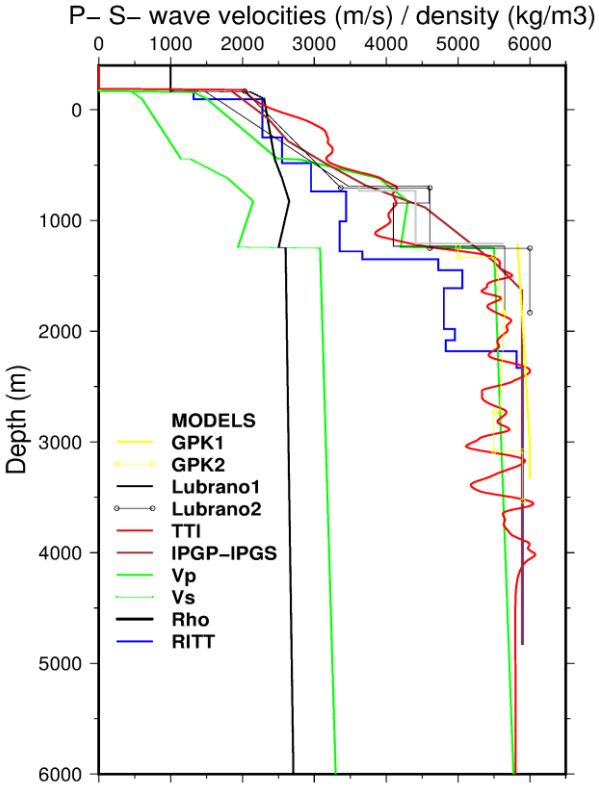

Figure 2: Compressional and shear velocities as well as density profiles collected from several sources. GPK1 and GPK2 are built from GPK4 welldata acquired in 2007. Lubrano's models are built from VSP data of Soultz (Lubrano 2013). TTI model is estimated from Travel Time Inversion using GPK4 welldata. IPGP-IPGS model is extracted from Horálek et al. (2010). Vp, Vs and Rho represent the values extracted from our 3D geological model for P-velocity, S-Velocity and density, respectively. The RITT model is built for Rittershoffen area (Maurer et al., 2016) located at only 8 km southeast of Soultz-sous-Forêts.

5.2 The inversion experiments

From the modeling experiments (section 5.1), we can note that the resulted seismic signal is significantly affected by the presence of the fault. Even if the modeled fault is narrow, only 20 m thick for 1 km long, the generated seismic effect is measurable. The exercise now is to check if the full wave inversion can retrieve the characteristics of the fault from the data.

Several parameters are required to insure the stability and the convergence of the inversion process. Among of them is to use an adequate velocities and density values. As our target show relatively a small reflectivity amplitude compared to a standard geological interface, it is important to use good starting velocity and density models. As the purpose of this paper is not to discuss the impact of the starting model, we started the inversion from the velocity and density models showed in Figure 3 but without the fault. In that case, the inversion process will be only focused on the fault imaging.

The antenna including 187 receivers in our experiment as well as the source position are those of the real data. After 100 iterations, we obtained models showed in Figure 5 for the reference inversion (spatial correlation of 50 m in both X and Z direction, diagonal covariance matrix on the data space). These results obtained using no noisy data and from a starting model which is close to the true model, show that this inverse problem is different from those in sedimentary contexts and need some tuning and also important improvement. The results for S-wave velocity and density are worse than expected, indicating that the freedom degrees in this reference inversion is too high compared to the information provided by the data. We consider that we could improve the results introducing cross parameters correlation. For instance, if the P-wave velocity should decrease due to the presence of a fault, then

the S-wave velocity as well and the density also. This feature is in development in the FWI code for further tests. The calculated data obtained from the estimated models, solution of the inversion, are shown in Figure 6. The comparison between seismograms clearly show that the observed data have been completely explained. The artefacts in the estimated models are therefore due to the underdetermination of the inverse problem.

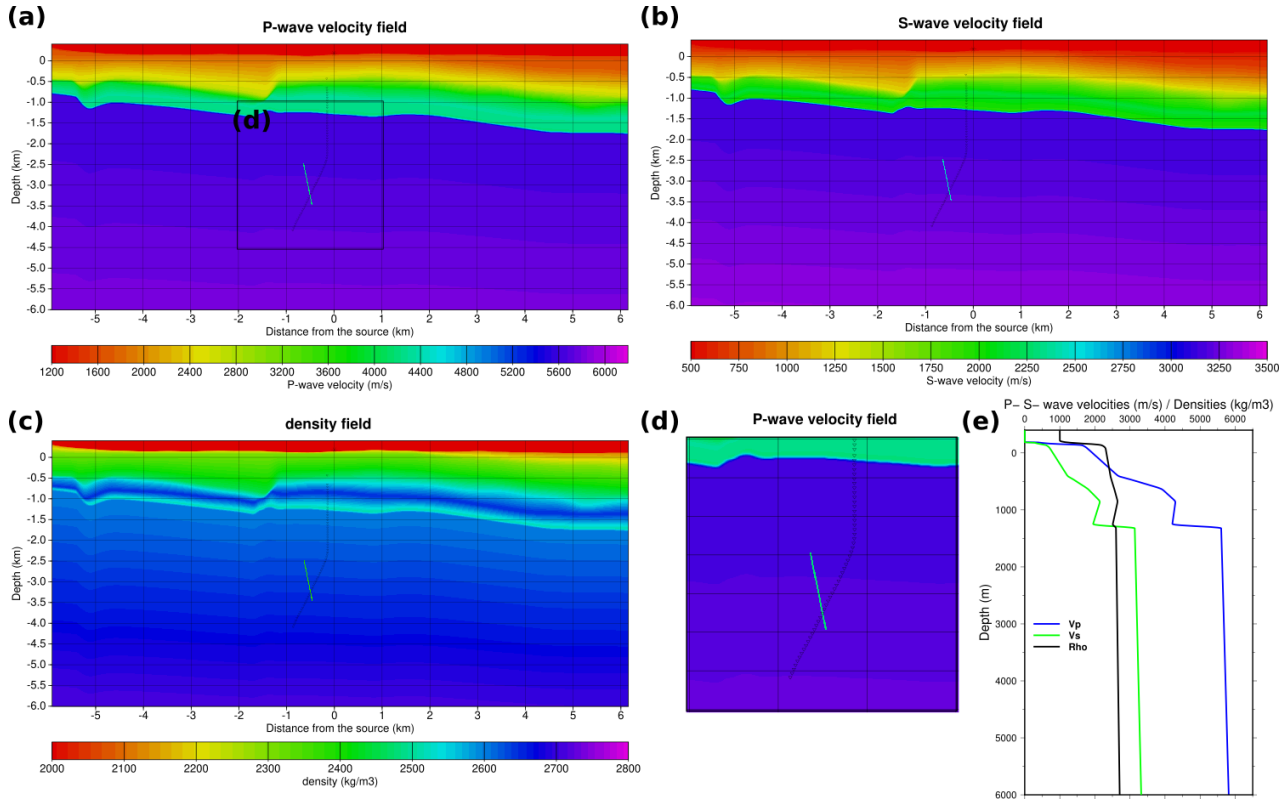

Figure 3: P- and S-wave velocities models and density models extracted from the true 3D model; a) P-velocity model, b) S-velocity model, c) density model, d) zoom into P-velocity model near the fault, and e) 1D P- and S-velocity models as well as density model according to the depth. These 1D curves are extracted at the origin of the model, which is the location of the source shown by an asterisk. The triangles denote the receiver locations. The fault clearly appears as its physical parameters Vp, Vs and rho are smaller. The thickness of the fault is 20 m and is subvertical (80 deg dip).

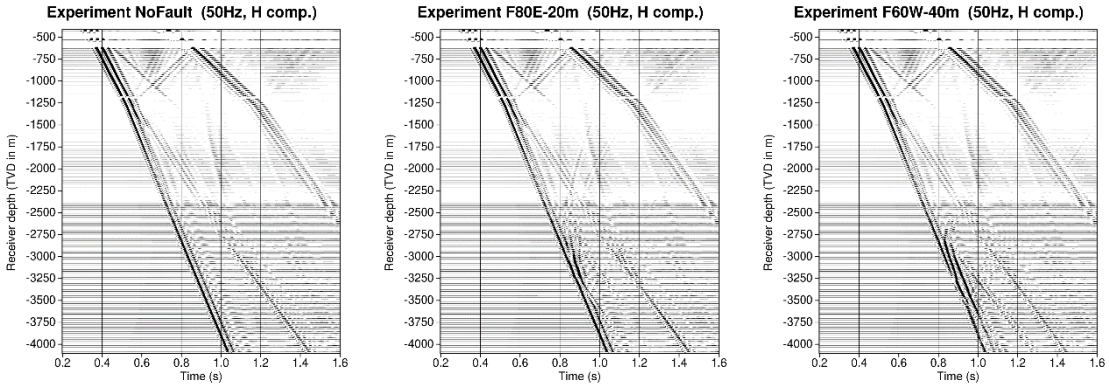

Figure 4: The horizontal components of the synthetic data are plotted for three modeling experiments. Left: no fault for reference; Middle: fault dipping east 80 deg with a thickness of 20m; Right: fault dipping west 30 deg with a thickness of 40 m. In both cases (middle, right), the fault crosses the well at 3200 m depth. The effect of the fault zone on the data is noticeable and different depending on the dip and other parameters. These results confirm that, even if the wavelengths are larger than the fault thickness, effects on data are sufficient to apply fullwave inversion to recover quantitative information from the data (when S/N ratio is sufficiently good).

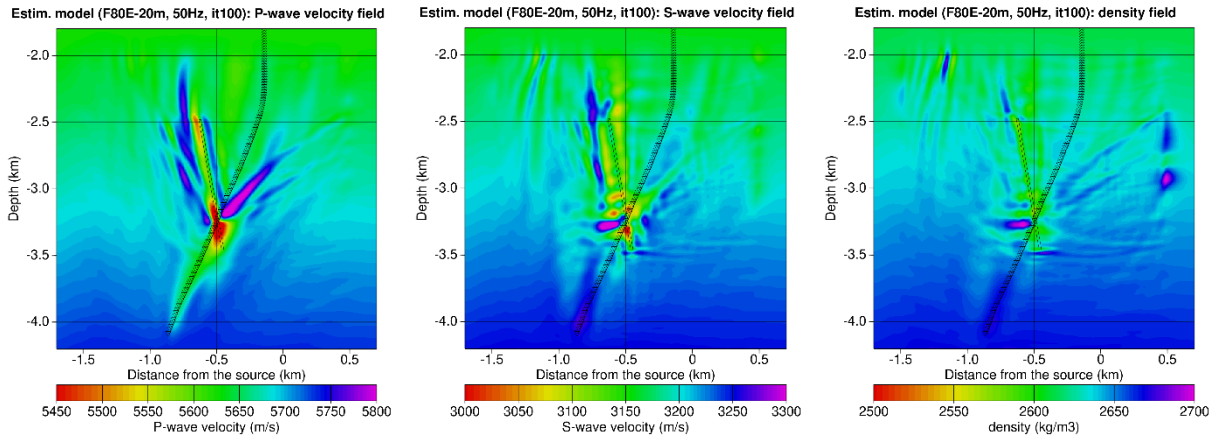

Figure 5: Results for the reference inversion experiment obtained after 100 iterations. The parameter fields are plotted for the zone of interest around the fault. Triangles denote the geophones while the true location of the fault is indicated by a rectangle drawn with a thin solid black line. Left: P-wave velocity estimated field; Middle: S-wave velocity estimated field and Right: density estimated field. Even if the inversion is able to find some structures, some strong artefacts are present, thus interpretation is not possible in that case. In addition, Vs and density field cannot be used.

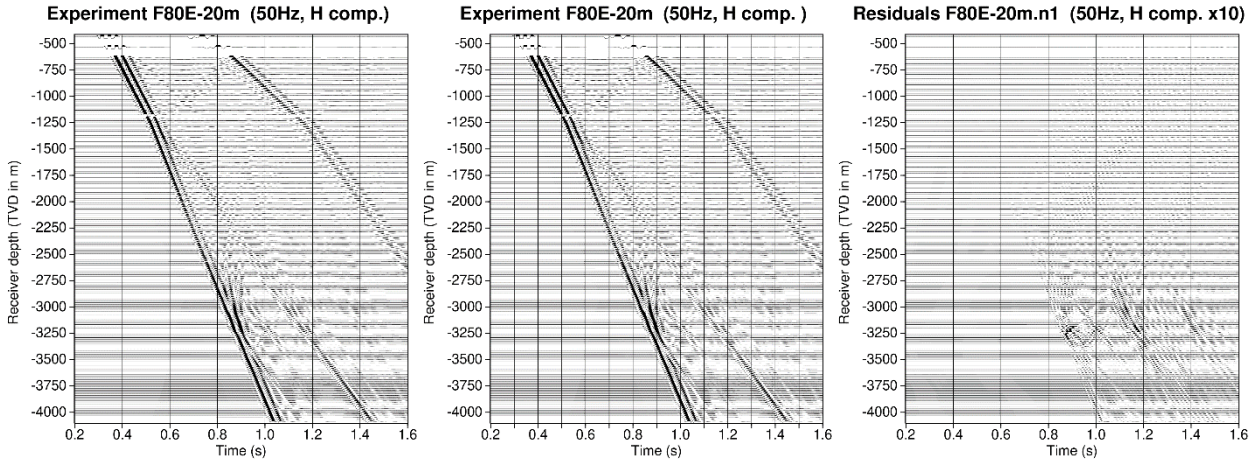

Figure 6: Seismograms for the reference inversion experiment, horizontal component. Left: the observed data (i.e. those obtained with the true model we want to retrieve); Middle: The calculated data from the estimated model after 100 iterations; Right: the residual data with amplitudes multiplied by 10. The difference between calculated data and observed data is very small after 100 iterations, showing that the most important part of the information contained in the data has been used. The estimated models, even with artefacts explain correctly the data, showing that artefacts are not due to noise or unsolved part of the data but to the fact the inverse problem is underdetermined.

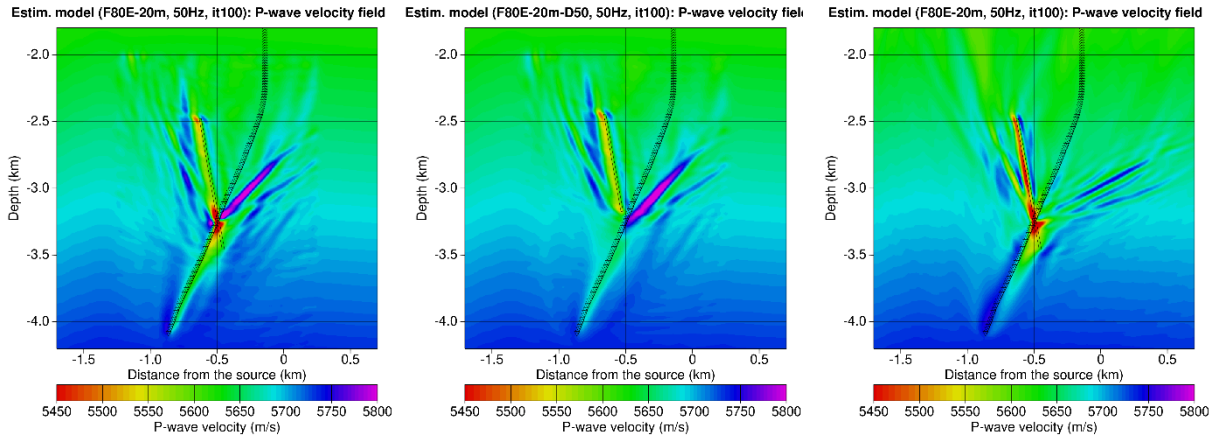

Figure 7: Results for 3 different inversion experiments, only the P-wave velocity estimated models are shown. Left: the inversion experiment using polarization of the data; Middle: the inversion experiment using polarization but for a fault which does not cross the well; Right: the inversion experiment when using 5 sources rather than one. Triangles denote the geophones while the true location of the fault is indicated by a rectangle drawn with a thin solid black line. Taking polarization into account (left) allows us to improve the results compared to the reference experiment

shown in Figure 5, the delineation of the fault is correct above the well trajectory and lateral artefacts are reduced, estimated values in the fault zone do not reach the correct one. For the case of a fault which does not cross the well, artefacts are about the same level, but the delineation of the fault is good, however, the estimated values in the fault zone are still too high. Using several sources (right) allows to obtain a quite good results as artefacts are smaller and the fault delineation correct with a better estimation of the parameter values in the fault zone.

The next step will be to adapt the inverse problem setting in order to better constrain the inverse problem, consistently with the goal of fault zone imaging.

In order to better understand the limits of the FWI for fault zone imaging, we have considered three other cases with the same fault geometry:

1. Including polarization constraint using a non-diagonal covariance matrix on the data space and using spatial correlation range of 20 m in both directions, vertical and horizontal, rather than 50 m done in the first experiment.
2. Including polarization of the data as well but for a shorter fault which does not cross the well trajectory, spatial correlation range is 20 m in both directions as well.
3. Using 5 sources rather than one, with distances of: -1000, -500, 0, 500 and 1000 m from the A0 vibrating point location with a spatial correlation range of 20 m as well.

The results for these additional experiments are shown in Figure 7.

5.3 Discussion from modeling and inversion synthetic experiments

The results of the modeling experiments show that the effects of a common fault zone as observed in the GPK4-A0 layout at least is noticeable and can be inverted to retrieve quantitatively its characteristics.

The results of the synthetic inversion experiments show that we can recover the location of the fault and its dimensions (Figure 5 and Figure 7). The fault delineation is not clear for all the parameter fields. Moreover, we note the presence of artefacts sufficiently important to lead to interpretation ambiguity of the obtained fields. The mitigation of these artefacts has been partially studied and the complementary inversion experiments show that the tuning of some parameters controlling the inversion, the use of additional constraints like polarization can help. As expected, the results are clearly improved when using five shots located at different offset (Figure 7). In addition, the P- and S-velocity recovered in the fault zone have decreased but are still overestimated when using one shot, however, it becomes very close to the true model when using several shots. We can remark also that the lower part of the fault, the part under the well trajectory, is recovered with less definition. This is due to its location according to the source location. Effectively, the receivers below the fault record a delayed signal due to the decrease of velocity in the fault zone. Thus, the traveltime increases for transmitted downgoing wave as the direct P-wave implying long wavelength features in the gradient field.

The studies of residuals data (Figure 6) show that the main part of the information contained in the data has been taken into account by the inversion process. The residuals are small and not very structured; as a consequence, we can say that the estimated fields obtained by the inversion, even containing artefacts, explain correctly the data. This result is important and shows that artefacts are not due to noise or unsolved part of the data but to the fact the inverse problem is underdetermined.

Therefore, we will focus our next efforts in constraining this underdetermined inverse problem consistently with the geological information and the expected characteristics of the fault zone. We have planned to introduce correlation between physical parameters. For the case of fault zones, the three parameters, i.e. P- and S-wave velocities and density decreases significantly and with a strong positive correlation as shown by log data, then a positive correlation between the fields is expected and can be introduced in the inversion process through the covariance matrix on the model space. Other improvement can be added still in order to reduce the degrees of freedom of the inversion, leading to a better determined stable inverse problem.

6. APPLICATION OF FWI ON REAL DATA

We have planned to apply the FWI to OVSP data acquired on Soultz-sous-Forêts survey of 2007. The first trials are in progress. We consider only the GPK4-A0 seismograms for the moment as the quality of the data is significantly better than for other shots. The data are presented in Figure 1. In a first step, we use a 2.5D FWI process. 2.5D means than the models (therefore the numerical grids) are 2D while the Green functions (impulsive response of the medium) is approximately 3D. A second step is planned using full 3D inversion as first, the fault plane is likely not perpendicular to the 2D propagation plane and second, the GPK4 well trajectory is not included in the 2D propagation plane, inducing errors in the inversion process and resulting in artefacts in the estimated fields.

We consider the 3D built model presented in section 4.2 as the starting model for the inversion. The multiscale approach uses first the low frequency of the data, and then increasing step by step. Four frequency ranges have been defined. The low frequency data are obtained by filtering the original data within a [8-20] Hz frequency band.

The elastic rheology seems sufficient at low frequency but, as the period of the wave is larger for deeper geophones, we suspect that attenuation has to be taken into account at higher frequency. In that case, we will use a viscoelastic rheology.

Only preliminary results for the low frequency band have been obtained for the moment. As the synthetic experiments show that additional developments have to be implemented (e.g. cross-correlation between parameters, see section 5), we have stopped the real data inversion. New developments should be available in the coming months.

7. CONCLUSION

In this study, we have modeled and inverted successfully synthetic VSP data. We have applied elastic modeling and invert the complete seismic wavefield. We deal with several challenges, as for instance, VSP data modeling including deviated well path.

Sensitivity study on fault imaging in Soultz-sous-Forêts context using modeling and inversion is presented and discussed. The effects of the fault on borehole seismic data have been evaluated by fullwave modeling. When the S/N ratio is not too low, it shows that effects are significant and can be interpreted quantitatively using the fullwave inversion method. We have considered a realistic fault extension and location as those found in Soultz. Although, we presented in this paper only a few synthetic tests, we performed several examples where different scenarios were studied, for instance the effect of the thickness of the fault, its dip and orientation etc, on the seismic data. All these tests confirm the detectability of the fault in granite context of Soultz-sous-Forêts.

The inversion results reflect the inversion challenges of this fault imaging. Even if we are able to recover velocities and density estimated fields comparable to the true models, the presence of some artefacts complexify somewhat the geological interpretation. We have shown that these artefacts are the consequence of the underdetermination of the inverse problem, partly due to the fact we use only one source location. Additional constraints consistent with the geological context and the characteristics of the fault zone should lead to a better determined inverse problem. A good tuning of the inversion algorithm should also improve the quality of the results.

The next steps are the following: The sensibility analysis based on synthetic inversion experiment will be completed. Some new features will be added to the inversion code in order to reduce the underdetermination of the problem. Finally, the method will be applied on the real OVSP data of Soultz survey of 2007.

ACKNOWLEDGMENTS

First of all, the authors thank EEIG “Heat Mining” for sharing geoscientific and technical data from Soultz-sous-Forêts geothermal site. Secondly, this work was realized within the MEET project which has received funding from the European Union’s Horizon 2020 research and innovation program under grant agreement No 792037.

REFERENCES

Abdelfettah, Y., Hinderer, J., Calvo, M., Dalmais, E., Maurer, V., Genter, A.,: Gravity versus thermal gradient: can we use gravity to discriminate potential hydrogeothermal area? European Geothermal Congress, EGC 2019, (2019b), 11-14 June 2019, The Hague, The Netherlands.

Abdelfettah, Y., Sailhac, P., Girard, J.-F., Dalmais, E., Maurer, V., Genter, A.: Resistivity image under GRT1-2 geothermal doublet of the Rittershoffen EGS project as revealed by magnetotelluric, Proceedings, European Geothermal Congress, EGC 2019, (2019a), 11-14 June 2019, The Hague, The Netherlands.

Aichholzer, C., Duringer, P., Orciani, S., Genter, A.,: New stratigraphic interpretation of the Soultz-sous-Forêts 30-year-old geothermal wells calibrated on the recent one from Rittershoffen (Upper Rhine Graben, France), Geotherm. Energy, 4(1), 13, (2016) https://doi.org/10.1186/s40517-016-0055-7

Barnes, C., and Charara, M.: Anisotropic anelastic full waveform inversion: Application to North Sea offset VSP data, 80th SEG Conference & Exhibition, Expanded abstracts, (2010), 972-976.

Barnes, C., and Charara, M.: Viscoelastic full waveform inversion of North Sea offset VSP data. 79th SEG Conference & Exhibition, Expanded abstracts, (2009), 2278-2282.

Baujard, C., Genter, A., Cuenot, N., Mouchot, J., Maurer, V., Hehn, R., Ravier, G., Seibel, O., Vidal, J.,: Experience from a successful soft stimulation and operational feedback after 2 years of geothermal power and heat production in Rittershoffen and Soultz-sous-Forêts plants (Alsace, France), in: Geothermal Resources Council Transactions, Reno, NE, USA. Oct. 14-17, (2018), 2241–2252.

Blanch, J.O., Robertsson, J.O.A. & Symes, W.W.,: Modeling of a constant Q: Methodology and algorithm for an efficient and optimally inexpensive viscoelastic technique, *Geophysics,* **60,** (1995), 176-184.

Charara, M., and Barnes, C.: Constrained Full Waveform Inversion for Borehole Multicomponent Seismic Data. Geosciences, 9(1), 45, (2019). https://doi.org/10.3390/geosciences9010045.

Charara, M., Barnes, C., and Tarantola, A.: The state of affairs in inversion of seismic data: an OVSP example. 66th SEG Conference & Exhibition, Expanded abstracts, (1996), 1999–2002.

Charara, M., Barnes, C., and Tarantola, A.: The state of affairs in inversion of seismic data: an OVSP example. *66th SEG Conference & Exhibition*, Proceedings, (1996), 1999–2002.

Christensen, R.M.,:Theory of viscoelasticity. Academic Press, New York, (1982).

Dezayes, C., Genter, A. and Valley, B.: Structure of the low permeable naturally fractured geothermal reservoir at Soultz. C.R. Geoscience, **342**, (2010), 517-530.

Dorbath, L., Cuenot, N., Genter, A., and Frogneux, M.: Seismic response of the fractured and faulted granite of Soultz-sous-Forets (France) to 5 km deep massive water injections. Geophysical Journal International, **177** (2), (2009), 653-675. ISSN 0956-540X

Edel, J.B., Whitechurch H. and Diraison M.: Seismicity wedge beneath the UpperRhine Graben due to backwards Alpine push?: Tectonophysics, **428**, (2006), 49-64.

Emmerich, H. and Korn, M.,: Incorporation of attenuation into time-domain computations of seismic wave fields, *Geophysics,* **52,** (1987), 1252-1264.

Genter, A., Castaing, C., Dezayes, C., Tenzer, H., Traineau, H. and Villemin, T.: "Comparative analysis of direct (core) and indirect (borehole imaging tools) collection of fracture data in the Hot Dry Rock Soultz reservoir (France)," Journal of Geophysical Research, **102**, no. B7, (1997), 15419–15431.

Genter, A., Evans, K., Cuenot, N., Fritsch, D. and Sanjuan, B.: Contribution of the exploration of deep crystalline fractured reservoir of Soultz to the knowledge of Enhanced Geothermal Systems (EGS). C.R. Geoscience, 342, (2010),502-516.

Genter, A., Traineau, H., Bourgine, B., Ledésert, B., and Gentier, S.: Over 10 years of geological investigations within the European Soultz HDR project, France. In: World Geothermal Congress 2000, Kyushu-Tohoku, Japan, May 28–June 10, (2000) 3707–3712.

Hirabayashi, N., and Leaney, W.: Velocity profile prediction using walkaway VSP data. *76th SEG Conference & Exhibition*, Proceedings, (2006), 3487-3491.

Horálek, J., Jechumtálová, Z., Dorbath, L. and Šílený, J.: Source mechanisms of micro-earthquakes induced in a fluid injection experiment at the HDR site Soultz-sous-Forêts (Alsace) in 2003 and their temporal and spatial variations, Geophys. J. Int., **181**, (2010), 1547–1565.

Leaney, W., Hornby, B.E., and Campbell, A.: Sub-salt velocity prediction with a lookahead AVO walkaway. *74th SEG Conference & Exhibition*, Proceedings, (2004), 2474-2476.

Lubrano, P.L.: Traitement des données de sismique de puits acquises en 2007 sur le site de Soultz-sous-Forêts pour la caractérisation de la fracturation du réservoir géothermique, PhD thesis, (2013), 1-158.

Maurer, V., Perrinel, N., Dalmais, E., Richard, A., Plévy, L., Genter, A. : Towards a 3D velocity model deduced from 2D seismic processing and interpretation in Northern Alsace (France). European Geothermal Congress 2016, EGC2016, (2016), 19-22 September 2016, Strasbourg, France.

Owusu, J.C., Podgornova, O., Charara, M., Leaney, S., Campbell, A., Ali, S., Borodin, I., Nutt, L., and Menkiti, H.: Anisotropic elastic full-waveform inversion of walkaway VSP data from the arabian Gulf. *Geophysical prospecting,* **64**(1), (2016), 38-53.

Place, J., Diraison, M., Naville, C., Géraud, Y.Schaming, Y., and Dezayes, C.: "Decoupling of deformation in the Upper Rhine Graben sediments. Seismic reflection and diffraction on 3-component vertical seismic profiling (Soultz-sous-Forêts area)," Comptes Rendus Geoscience, **342**, **7-8**, (2010), 575–586.

Podgornova, O., and Charara, M.: Multiscale time-domain full-waveform inversion for anisotropic elastic media. *81th SEG Conference & Exhibition*, Proceedings, (2011), 2459-2464.

Polack, E., and Ribière, G.: Note sur la convergence de méthodes de directions conjuguées. Revue française d'informatique et de recherche opérationnelle. 16-R1, (1969), 35-43.

Pribnow, D. and Schellschmidt, R.: Thermal tracking of Upper crustal fluid flow in the Rhine Graben. *Geophys. Res. Lett*, **27**, (2000), 1957-1960.

Reiser, F., Schmelzbach, C., Maurer, H., Greenhalgh, S., and Hellwig, O. : Optimizing the design of vertical seismic profiling (VSP) for imaging fracture zones over hardrock basement geothermal environments. Journal of Applied Geophysics, **139**, (2017), 25-35.

Richard, A., Gillot, E., Maurer, & V., Klee, J.: "Northern Alsace (France): the largest geothermal exploration by 3D seismic reflection, European Geothermal Congress, EGC 2019, 11-14 June 2019, (2019), The Hague, The Netherlands.." European Geothermal Congress 2019

Sanjuan, B., Millot, R., Innocent, Ch., Dezayes, Ch., Scheiber, J. and Brach, M.: Major geochemical characteristics of geothermal brines from the Upper Rhine Graben granitic basement with constraints on temperature and circulation, *Chemical Geology,* **428,** (2016), 27–47.

Sausse, J., Dezayes, C., Dorbath, L., Genter, A., and Place, J. (2010). 3D fracture zone network at Soultz based on geological data, image logs, microseismic events and VSP results. C.R. *Geoscience,* 342, pp. 531-545.

Sittler, C.,: Le pétrole dans le département du Haut-Rhin. Bilan d'un siècle et demi de recherches et d'exploitation, Bull Sci Géol, **25**, 2-3, (1972), 151–161, Strasbourg (in French language)

Tarantola, A: Inverse Problem Theory: Methods for data fitting and model parameter estimation: Elsevier, (1987).

Tarantola, A.,:Theoretical background for the inversion of seismic waveforms including elasticity and attenuation, *Pure and Applied Geophysics,* **128,** (1988), 365-399.

Valley, B.C., and Evans,K. F.,: "Stress state at Soultz-sous-Forêts to 5 km depth from wellbore failure and hydraulic observations, Proceedings of Thirty-Second Workshop on Geothermal Reservoir Engineering. Stanford University, California, USA, (2007).